Internal Tooth Structure and Burial Practices: Insights into the Neolithic Necropolis of Gurgy (France, 5100-4000 cal. BC)

Mona Le Luyer[1]*, Michael Coquerelle[2], Stéphane Rottier[1], Priscilla Bayle[1]

1 Unité Mixte de Recherche 5199, de la Préhistoire à l'Actuel: Culture, Environnement, Anthropologie (UMR 5199 PACEA), Université de Bordeaux, Pessac, France, 2 Department of Oral Surgery, Rey Juan Carlos University, Alcorcon, Spain

* mona.le-luyer@u-bordeaux.fr

Abstract

Variations in the dental crown form are widely studied to interpret evolutionary changes in primates as well as to assess affinities among human archeological populations. Compared to external metrics of dental crown size and shape, variables including the internal structures such as enamel thickness, tissue proportions, and the three-dimensional shape of enamel-dentin junction (EDJ), have been described as powerful measurements to study taxonomy, phylogenetic relationships, dietary, and/or developmental patterns. In addition to providing good estimate of phenotypic distances within/across archeological samples, these internal tooth variables may help to understand phylogenetic, functional, and developmental underlying causes of variation. In this study, a high resolution microtomographic-based record of upper permanent second molars from 20 Neolithic individuals of the necropolis of Gurgy (France) was applied to evaluate the intrasite phenotypic variation in crown tissue proportions, thickness and distribution of enamel, and EDJ shape. The study aims to compare interindividual dental variations with burial practices and chronocultural parameters, and suggest underlying causes of these dental variations. From the non-invasive characterization of internal tooth structure, differences have been found between individuals buried in pits with alcove and those buried in pits with container and pits with wattling. Additionally, individuals from early and recent phases of the necropolis have been distinguished from those of the principal phase from their crown tissue proportions and EDJ shape. The results suggest that the internal tooth structure may be a reliable proxy to track groups sharing similar chronocultural and burial practices. In particular, from the EDJ shape analysis, individuals buried in an alcove shared a reduction of the distolingual dentin horn tip (corresponding to the hypocone). Environmental, developmental and/or functional underlying causes might be suggested for the origin of phenotypic differences shared by these individuals buried in alcoves.

Introduction

Traditionally, biological affinities and kinship between populations and individuals are approached by the analysis of crown size and shape, using external diameters and non-metric variations [1–15]. Crown size and shape are influenced by genetic, epigenetic and environmental factors (see [16,17] for an overview). Whereas the polygenetic control is relatively strong [5,17–21] and seems to be dominant for crown size [18], the impact of environmental factors on tooth variations has been demonstrated, notably by the studies of twins [19,22–25]. In addition, the buccolingual diameter is less influenced by environmental factors than the mesiodistal diameter [26], suggesting a different genetic control between these two dimensions [27,28]. Non-metric variations are also determined by multiple factors, which are under moderate to high-genetic and environmental controls [7,29–31]. They are considered as reliable markers for measuring biological relatedness and thus widely used to estimate biological relationships between populations and affinities between individuals [9,11,31–46].

Community-shared or family-centered practices might influence the organization of the necropolises, this means that burial practices may reflect the social composition of the population [31,33,47]. Morphological and genetic methods are generally applied in order to characterize biological relationships between individuals in burial grounds. It is possible to identify closely related individuals but the precise genealogical degree of this kinship is rarely specified.

Because of the high heritability of non-metric variations [16,31], these phenotypic data are studied in order to assess the social structure of necropolises [31,44,47–49]. In particular, teeth are often singled out for their potential to identify biological relatives [50–52] and even siblings [15]. More recently, advances in paleogenetics allow to compare cemetery organization and kinship from ancient DNA analysis, also with some precise genetic affiliation [53–56]. Affinities obtained from these two methods–non-metric and genetic–are correlated [57–59]. Paleogenetic analyses are destructive and dependent on the preservation of the remains–ancient DNA may not be conserved. So far, external morphometric analyses of the crown are used to assess biological affinities, providing information that describes in essence the macrostructural outcomes of dental development.

At meso- and microstructural level, teeth record a wealth of unique information within their tissues that are crucial in bioarcheology and paleoanthropology [60–80]. Enamel thickness, crown tissue proportions and enamel-dentin junction (EDJ) shape have been shown as relevant parameters to finely characterize taxonomy, phylogenetic relationships, dietary and/or developmental patterns [62–69,81–95]. The EDJ, which is the interface between the enamel cap and crown dentin [96] and the developmental precursor and primary contributor to the outer morphology of the crown [65,91,92,97,98], has been shown to successfully discriminate hominoid species [62,65,91,92,99–102]. Moreover, the EDJ is morphologically more conservative than the outer enamel surface and provides essential information about the developmental processes underlying tooth crown growth [65,100,102]. According to the inhibitory cascade model of development [103], the morphology of the crown is an iterative process determined by a morphodynamic interaction between developmental genes and cusps morphogenesis. This model predicts the future cusp size and shape, the number of cusps [104–107] as well as the pattern of tooth sizes for the lower postcanine teeth [108].

Advanced virtual imaging techniques, that are non-invasive methods, allow such quantitative and qualitative characterizations of internal structures. However, at a microevolutionary scale, these variables have been poorly assessed in modern humans to discuss inter- or intrapopulational variability [109,110]. While the study of internal tooth structure may help to assess subtle phenotypic differences across/within archeological assemblages, in our knowledge, the use of internal tooth structure is original to characterize the variations at the intrasite scale.

More importantly, in addition to provide precise phenotypic assessment, internal tooth structure analyses may allow to understand the developmental, functional and phylogenetic underlying causes of these variations.
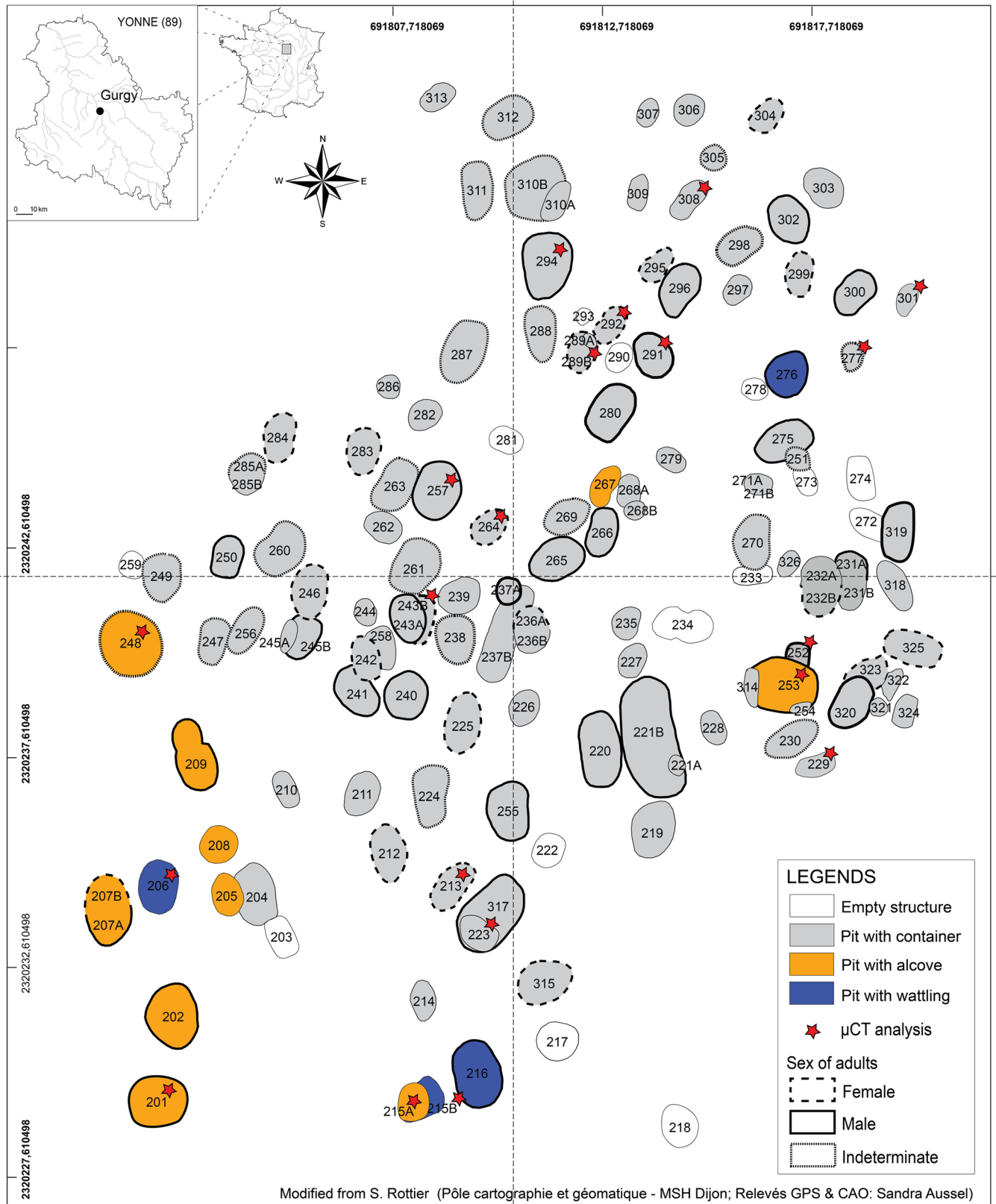
The Neolithic necropolis of Gurgy

Discovered in 1997 in the southern Paris Basin (Yonne, France), excavations at Gurgy yielded 128 individuals (**Fig 1**), which make the site one of the most important necropolises currently known for the Early/Middle Neolithic transition in Western Europe [111,112]. Among the 134 pits dug in Gurgy, 120 were identified as primary burials: individual structures were largely dominant and few were double burials. Both individual and double burials present various funerary architectures [112], including pits with evidence of a container in perishable material (container), pits with a wattle-like construction on the walls (wattling) and pits with a lateral overdigging where the body was deposited (alcove, see **S1 Fig**). The majority of the bodies were positioned on the left side, with the head to the south or the south-west, upper limbs hyper-flexed and lower limbs either bended or hyperbended [113]. Some grave goods were found associated with the individuals buried at Gurgy: animal bones or teeth, shells, flint, ochre and rare pottery [111]. Radiocarbon dates of human remains range between 5100–4000 cal. BC (see [114]) and represent a continuous use of the necropolis for a thousand years. Three main chronological phases of occupation of the site could be identified: the principal phase (B) with the most intensive use is ranged from 4800 and 4500 cal. BC, is framed by an early phase (A) before 4800 cal. BC and a recent phase (C) dated after 4500 cal. BC (see **S2 Fig**).

The necropolis of Gurgy is situated at the confluence of the two migration routes of the European Neolithization, in the culturally rich and complex archeological area of the Paris Basin during the transition from the Ancient to the Middle Neolithic. Given these multiple cultural influences are visible at Gurgy [111,112], it is not possible to propose a specific cultural attribution ([113,114] see in particular the Supplementary Informations). Indeed, for the period and the region, Gurgy revealed a more homogeneous and inconspicuous funerary profile: a necropolis without monument and any structuring of funerary space [44,115]. Paleogenetic analyses show equivalent genetic contributions of the two European neolithization waves in Gurgy population, revealing the most ancient mixture between farmers from both Danubian and Mediterranean migration routes [114]. At the intrapopulation scale, even if ancient DNA was not conserved in all sampled individuals and no Y chromosome DNA was found, and thus no precise degrees of kinship were discussed, some individuals sharing mitochondrial DNA haplotypes and archeological and spatial features might be closely maternally related [114,116].

According to the analyses conducted so far, the Gurgy population is homogeneous regarding isotopic variation [117], enamel thickness topography and tooth wear patterns [93]. Although influenced by the rich cultural diversity of the Paris Basin [113,114], the funerary practices at Gurgy are rather homogeneous [113]. All these data suggest that the necropolis was used by a uniform population (even if genetically derived from both Neolithization waves) sharing a common cultural framework.

Aims of the study

In this study, a high resolution microtomographic (microCT)-based record of upper permanent second molars from Neolithic individuals of the necropolis of Gurgy was applied with the aim to evaluate intrasite variation in crown tissue proportions, thickness and distribution of enamel, and enamel-dentin junction shape. This study explore subtle phenotypic dental variation and its underlying causes among individuals buried at Gurgy. Using these internal tooth

Fig 1. Map of the Neolithic necropolis of Gurgy (Yonne, France).

doi:10.1371/journal.pone.0159688.g001

structure parameters and facing these data against burial practices and chronocultural parameters, this investigation will address the following questions:

- Do phenotypic distances obtained from the study of morphological and metrical variation of internal tooth structure are a reliable proxy to track groups sharing similar chronocultural and burial practices?

- Is one of these internal parameters more relevant to discuss interindividual variability?

- Can causes of dental variations be suggested?

Materials and Methods

Samples

For this preliminary study, 20 upper permanent second molars (UM2) were examined for 13 adults (whom 6 males, 5 females, and 2 indeterminate) and 7 immature individuals from Gurgy (**Table 1**), all buried in primary structures (**Fig 1**). UM2 have been selected because they are often less worn than M1, and their development is more correlated to somatic and sexual maturation than those of M3 [118]. Crowns are complete (at least, maturational stage D and further [119]) and well-preserved, exempt from caries, pathologies and damages. Dental wear patterns were recorded according to the procedure of Molnar [120] and teeth range from unworn to slightly worn (**Table 1**). Age-at-death estimation was based on dental development [121,122], bone ossification and diaphyseal length [123] and chronological metamorphosis of the auricular surface of the ilium [124]. Sex was assessed using the morphology and morphometry of the *ossa coxae* [125–127]. Details on sample composition regarding biological and chronocultural parameters are given in **Table 1,** and summarized on the necropolis map (**Fig 1**). Direct radiocarbon ages of human remains were available for a large sample of individuals in the necropolis (calibrated at 2 sigmas with OxCal 4.2.4 [128] and curve IntCal13 [129], see also **S2 Fig**)

Microtomographic record

The UM2 were scanned on Skyscan 1076 X-ray equipment set at the MRI platform (University Montpellier 2, France). Acquisitions were realized according to the following parameters: 100 kV voltage, 100 μA current, a 1.0 mm aluminum filter and a rotation step each 0.20°. The software Nrecon v1.6.6 (Skyscan) was used to reconstruct the final volumes with an isotropic voxel size ranging from 17.93 μm for isolated teeth to 36.18 μm for jaw fragments. Following the half-maximum height method [130,131], a semi-automatic threshold-based segmentation with manual corrections was conducted using Avizo v.7 (VSG) [62,84–87,89,94,132–135]. Crowns were digitally isolated from roots [85] and three-dimensional (3D) surface models were generated using a constrained smoothing algorithm. All 3D surface models were deposited in MorphoMuseuM [136].

Dental tissue proportions and enamel thickness analysis

Using MPSAK v2.9 (developed by L. Bondioli, available in [137], seven 2D variables were measured or calculated on virtual buccolingual cross-sections realized through the dentin horn tips of the mesial cusps (see **S3 Fig**): total crown area (a, mm^2); enamel area (c, mm^2); coronal dentin and pulp area (b, mm^2); percentage of crown area that is dentin and pulp (%b, %); enamel-dentin junction (EDJ) length (e, mm); 2D average enamel thickness (AET2D (= c/e), mm) and 2D relative enamel thickness (RET2D (= AET2Dx100/(b)$^{1/2}$), scale-free) [81,86]. For lightly worn crowns, 2D corrections of outer enamel surface were made prior to measurements of the

Table 1. The 20 Neolithic individuals sampled in the necropolis of Gurgy. Details of biological (age and sex, maturational and wear stages, mtDNA haplogroups) and chronocultural parameters (radiocarbon age, phase, burial structure, orientation and location in the necropolis).

Individual [1]			Teeth			mtDNA	Burial			Ages	
Number	Age [2]	Sex [2]	UM2	Maturational stage [3]	Wear stage [4]	Haplogroug [5]	Structure [6]	Orientation	Location	14C cal. BC	Phase [7]
201	16–18	M	left	H	2	K	Alcove	E_W	SW	5206–4840	A
206	3.5–7		left	D	1		Wattling	N_S	SW		
213	15–29	F	right	H	2		Container	NE_SW	SW	4937–4728	B
215A	4–8		right	D	1		Alcove	NW_SE	SW		B
215B	8–14		right	E	1	J1	Wattling	N_S	SW		
223	4–7		right	D	1	U5	Container	N_S	SW	4770–4536	B
229	12–19		right	H	1	K	Container	SW_NE	SE		C
243B	>20	F	left	H	3	X	Container	N_S	SW	4828–4609	B
248	>40	I	left	H	3	U5	Alcove	N_S	SW	4313–3991	C
252	>30	M	left	H	1		Container	N_S	SE	4763–4536	B
253	20–59	M	left	H	2		Alcove	NE_SW	SE	4235–3991	C
257	>30	M	right	H	3		Container	NE_SW	NW	4841–4556	B
264	15–29	F	left	H	2	H1	Container	NE_SW	NW		
277	15–29	I	right	H	2	J	Container	N_S	NE		
289B	>30	F	right	H	1	K	Container	SW_NE	NE	4770–4489	B
291	>30	M	right	H	3		Container	NE_SW	NE		B
292	20–29	F	right	H	1	H1	Container	SW_NE	NE		B
294	>20	M	left	H	2	U5	Container	E_W	NE		B
301	6–12		left	E	1	K	Container	NE_SW	NE	4763–4536	B
308	9–14		right	G	1		Container	NE_SW	NE		

[1] The original specimens are deposited in the Ostéothèque de Pessac (Université de Bordeaux). All material included is archeological; no permits were required for the described study.

[2] Revised from [113,114]; personal communications and observations; M = male; F = female; I = indeterminate.

[3] According to Demirjian et al. [119], D = the crown formation is completed down to the enamel-dentin junction; E = the root length is still less than the crown height; F = the root length is equal to or greater than the crown height; G = the walls of the root canal are parallel and its apical end is still partially open; H = the apical end of the root canal is completely closed.

[4] According to Molnar [120], 1 = unworn teeth; 2 = minimal wear facets; 3 = small dentin patches.

[5] All individuals were selected for mitochondrial DNA (mtDNA) analysis, unfortunately, not all samples yielded results. See Rivollat et al. [114].

[6] Burial pictures are provided in S1 Fig. See Rottier [112] for description.

[7] A: early phase (before 4800 cal. BC); B: principal phase (4800–4500 cal. BC); C: recent phase (after 4500 cal. BC). See also S2 Fig.

doi:10.1371/journal.pone.0159688.t001

AET2D and RET2D values: reconstructions of the removed enamel were performed based on morphology observed for unworn teeth [69].

Height variables describing 3D dental tissue proportions were digitally measured or extracted using Avizo v.7 (VSG) on the crown reconstructions (see S4 Fig): total crown volume (Cvol, mm^3); enamel volume (Evol, mm^3); coronal dentin volume (Dvol, mm^3); coronal dentin and pulp volume (DPvol, mm^3); percentage of crown volume that is dentin and pulp (%DPvol, %); EDJ surface area (S_{EDJ}, mm^2); 3D average enamel thickness (AET3D (= Evol/S_{EDJ}), mm) and 3D relative enamel thickness (RET3D (= AET3Dx100/(DPvol)$^{1/3}$), scale-free) [62,83–85]. While enamel thickness increases allometrically with body and/or tooth size, RET3D allows comparisons between specimens with different body size [81].

The topographic variation of standardized enamel thickness (see S3 Fig) was measured using MPSAK v2.9 [137] in buccal and lingual aspects of the virtual buccolingual cross-sections [93,138]. In order to calibrate enamel thickness values and allow comparisons independent to tooth size and occlusal wear, the bi-cervical diameter (BCD) was defined at 10 mm (S3 Fig)

prior to digitize thicknesses between enamel-dentin junction and outer enamel surface, from the neck to the apex with an interval of 0.25 mm [93,138].

Three-dimensional maps of the topographic distribution of enamel thickness were created by measuring the distance between the outer enamel surface and enamel-dentin junction [64]. Differences in enamel thickness were rendered by a thickness-related, pseudo-color scale ranging from dark blue for thinner enamel to red for thicker enamel.

Estimated intra- and interobserver error rates were lower than 5% in all measured variables. The non-parametric Mann–Whitney U-test was employed to evaluate differences between the sexes and between individuals sharing cultural parameters. Plots of AET against b or DPvol, respectively in 2D and in 3D, were used to illustrate the relationship between AET and tooth size. Cluster analyses were performed on 2D and 3D tissue proportions using Ward's hierarchical clustering method [139], with a bootstrap of 1000 repetitions.

Geometric morphometric analysis of EDJ shape

Using the software Viewbox 4 (dHAL software, Kifissia, Greece), a 3D template of 114 points was created with an assemblage of three sets of 3D landmarks (**S5 Fig**). Compared to studies aiming to assess variations at a macroevolutionary scale [91,95], a large number of landmarks and semilandmarks was placed in order to finely quantify morphological EDJ variations in a microevolutionary context. The first set includes five anatomical landmark points: four were digitized on the tip of the dentin horn of corresponding four main cusps (i.e. protocone, paracone, metacone, hypocone) and one on the maximum lower part of the occlusal basin. Although unworn to slightly worn UM2 were selected, four teeth exhibit small dentin patches. Based on morphology observed for preserved dentin horns, reconstructions of the apex of dentin horn tips were made using Avizo v.7 (VSG), prior to digitally place landmarks. The second set is composed of 52 curve semilandmarks: 17 were digitized along the top of the ridges which connected the three dentin horns of the protocone, the paracone and the metacone, five were digitized along the ridge between the metacone and the hypocone, and 30 were collected along the cervix of the tooth crown. The third set includes 57 surface semilandmarks distributed uniformly over the occlusal basin and the wall of the EDJ surface [91,101,140–143].

Using Viewbox 4 (dHAL), the template was warped onto each specimen's EDJ surface by a thin-plate spline (TPS) interpolation function, and points were projected onto the targeted EDJ surface. As part of the digitization process, semilandmarks were allowed to slide along the curves and surfaces in order to minimize the bending energy of the TPS computed between each EDJ specimen and the Procrustes average shape [140,144]. After sliding, landmarks and semilandmarks were treated as homologous points [140] and converted to shape coordinates by Generalized Procrustes Analysis [144–146]. This involves rescaling the landmark coordinates so that each configuration has a unit Centroid Size (CS). Next, all configurations were translated and rotated to minimize the overall sum of the squared distances between corresponding (semi)landmarks.

Using R ([147], packages Morpho, shapes, scatterplot3d), a Principal Component Analysis (PCA) was carried out on the matrix of shape coordinates augmented by a column of the natural logarithm of Centroid Size (LnCS)–corresponding to a PCA in form space [148]. PC1 usually captures overall size variation as well as size-related shape variation (allometry), whereas the other PCs contain residual, non-allometric, shape variation and are weakly correlated with size.

A 3D digital EDJ surface was warped towards the Procrustes mean form using a thin plate spline (TPS) interpolation function using Avizo v.7 (VSG). Thereafter, the surface of the Procrustes mean configuration (consensus) was used to visualize size and shape variation along

the PCs. The shape deformation represented by the eigenvectors of a particular PC was visualized as a TPS deformation from the consensus plus or minus the eigenvectors (right and left sides of the PC, respectively). Once the eigenvectors (those related to the shape variables) are added or subtracted from the consensus, all variables are also multiplied by the exponent of the eigenvector for LnCS [149].

Results

Dental tissue proportions and enamel thickness

For each individual, 2D variables measured on virtual buccolingual sections–and corrected for occlusal wear–are presented in Table 2. While males tend to have higher 2D tissue proportions, in particular higher dentin surface (Table 3, see also S6 Fig), no significant differences were found between sexes, burial structures and occupation phases of the necropolis. In majority, the same information is found with 3D and 2D crown variables, but plots of 2D tissue proportions show slightly more nuanced differences between burials and between phases (Fig 2). Indeed, only the males buried in a pit with alcove (individuals 201 and 253) fall out of the variability shown by individuals buried in a pit with container (Fig 2 left), while individual 248 which is from the recent phase appears to be included in the variability of individuals from the main phase (Fig 2 right).

All 3D variables measured for upper permanent second molars (UM2) of each specimen are presented in Table 4 and descriptive statistics are detailed in Table 5. Reconstructions of 3D

Table 2. Measured 2D variables of crown tissue proportions for each individual.

Individual	a	c	b	%b	e	AET2D	RET2D
201	72.19	25.21	46.98	65.08	20.66	1.22	17.80
206	61.58	25.53	36.05	58.54	18.53	1.38	22.95
213	57.90	23.61	34.29	59.22	18.40	1.28	21.91
215A	54.16	24.06	30.10	55.58	17.72	1.36	24.75
215B	62.53	26.37	36.16	57.83	19.75	1.34	22.20
223	59.41	25.68	33.73	56.77	18.09	1.42	24.45
229	68.17	25.34	42.83	62.83	20.51	1.24	18.88
243B	55.32	19.52	35.80	64.71	18.20	1.07	17.93
248	53.67	22.99	30.68	57.16	19.65	1.17	21.12
252	62.77	21.06	41.71	66.45	20.34	1.04	16.04
253	75.97	25.65	50.32	66.24	21.64	1.19	16.71
257	66.19	25.03	41.16	62.18	20.35	1.23	19.17
264	60.31	19.79	40.52	67.19	20.18	0.98	15.41
277	60.64	25.19	35.45	58.46	20.28	1.24	20.86
289B	51.30	22.44	28.86	56.26	16.45	1.36	25.39
291	48.52	18.66	29.86	61.54	17.04	1.09	20.04
292	60.15	24.92	35.23	58.57	18.94	1.32	22.17
294	53.11	16.33	36.79	69.26	18.11	0.90	14.87
301	52.58	26.01	26.57	50.53	17.01	1.53	29.66
308	56.44	23.29	33.15	58.73	17.78	1.31	22.75

a = total crown area (mm^2)

c = enamel area (mm^2)

b = coronal dentin and pulp area (mm^2)

%b = percentage of crown area that is dentin and pulp (%)

e = enamel-dentin junction length (mm)

AET2D = 2D average enamel thickness (mm)

RET2D = 2D relative enamel thickness (scale free).

Table 3. Descriptive statistics of 2D measured variables for all individuals, female and male individuals, separately.

		a	c	b	%b	e	AET2D	RET2D
All individuals	mean ± SD	59.64 ± 7.06	23.33 ± 2.84	36.31 ± 6.11	60.66 ± 4.74	18.98 ± 1.45	1.23 ± 0.16	20.75 ± 3.77
	range	48.52–75.97	13.66–26.37	26.57–50.32	50.53–69.26	16.45–21.64	0.90–1.53	14.87–29.66
	CV	0.12	0.12	0.17	0.08	0.08	0.13	0.18
Female	mean ± SD	57.00 ± 3.77	22.06 ± 2.36	34.94 ± 4.16	61.19 ± 4.57	18.43 ± 1.35	1.20 ± 0.17	20.56 ± 3.91
	range	51.30–60.31	19.52–24.92	28.86–40.52	56.26–67.19	16.45–20.18	0.98–1.36	15.41–25.39
	CV	0.07	0.11	0.12	0.07	0.07	0.14	0.19
Male	mean ± SD	63.16 ± 10.68	21.99 ± 3.92	41.14 ± 7.28	65.12 ± 2.88	19.69 ± 1.74	1.11 ± 0.13	17.44 ± 1.95
	range	48.52–75.97	16.33–25.65	29.86–50.32	61.54–69.26	17.04–21.64	0.90–1.23	14.87–20.04
	CV	0.17	0.18	0.18	0.04	0.09	0.12	0.11

For the definitions of the abbreviated variables, see **Table 2**.

surface models for enamel and dentin components are shown **S7 Fig**, which allows to compare the morphology between the UM2 crowns.

The results show an overall biological proximity in enamel thickness and dental tissue proportions for individuals buried at Gurgy. Males show greater quantity of each tissue than females (**Table 5**). From Mann-Whitney U-test, only the volume of dentin (Dvol) is significantly higher for males than for females (p = 0.045). Proportion of these tissues into the crown (%DPvol) is comparable between sexes. No significant differences were found between individuals buried in different burials structure or individuals from different phases of the necropolis. However, while relatively low range of variation is shown in dental tissue proportions and enamel thickness for individuals of Gurgy (**Fig 3**), males tend to have higher crown tissue proportions than females (see also **S8 Fig**). Also, even if occlusal wear slightly affects enamel volume (Evol), grouping of individuals based on tissue proportions and thickness show an overall correlation with chronocultural parameters (**Fig 3**). Individuals buried in pit with wattling are systematically included in the variability shown by those buried in pit with container, whereas individuals buried in alcove are out of this variability, in particular individual 201 and 248. Moreover, individuals buried in a pit with wattling (206-215B) are very close and share high proximity in crown tissue proportions (Evol and DPvol, **Fig 3** **top left**) and enamel thickness (**Fig 3** **bottom left**), while those buried in pit with alcove present the highest variability (individuals 248-215A and 201 are at extreme opposition, respectively, **Fig 3** **left**). Also, individuals from the early phase (A) and the recent phase (C) of the necropolis use are out of the biological variability observed for individuals from the principal occupation of the necropolis (phase B, **Fig 3** **right**). Particularly, individual 201 from the oldest phase exhibits the most different condition, as he presents the highest value for both Evol and DPvol (**Fig 3** **top right**) and EDJ surface (**Fig 3** **bottom right**).

Measurements of topographic variation in enamel thickness allow comparisons which are not affected by occlusal wear. For all individuals, enamel is thicker on the lingual aspect than on the buccal aspect (**Fig 4**). Individuals buried in a pit with alcove show a more homogeneous enamel thickness distribution between lingual and buccal aspects of the crown, and present systematically thinner enamel on the lingual aspect than other individuals (**Fig 4**).

The dendrogram obtained from the application of Ward's method to 3D variables is presented in **Fig 5**. The intercluster distance values are relatively small, suggesting a high homogeneity within the population. Whichever the dataset used (see **S9 Fig** and **S10 Fig** for cluster analyses performed on 2D variables, on enamel and on dentin components, separately), the results of cluster analysis could be divided into two main clusters. In a large majority, the same
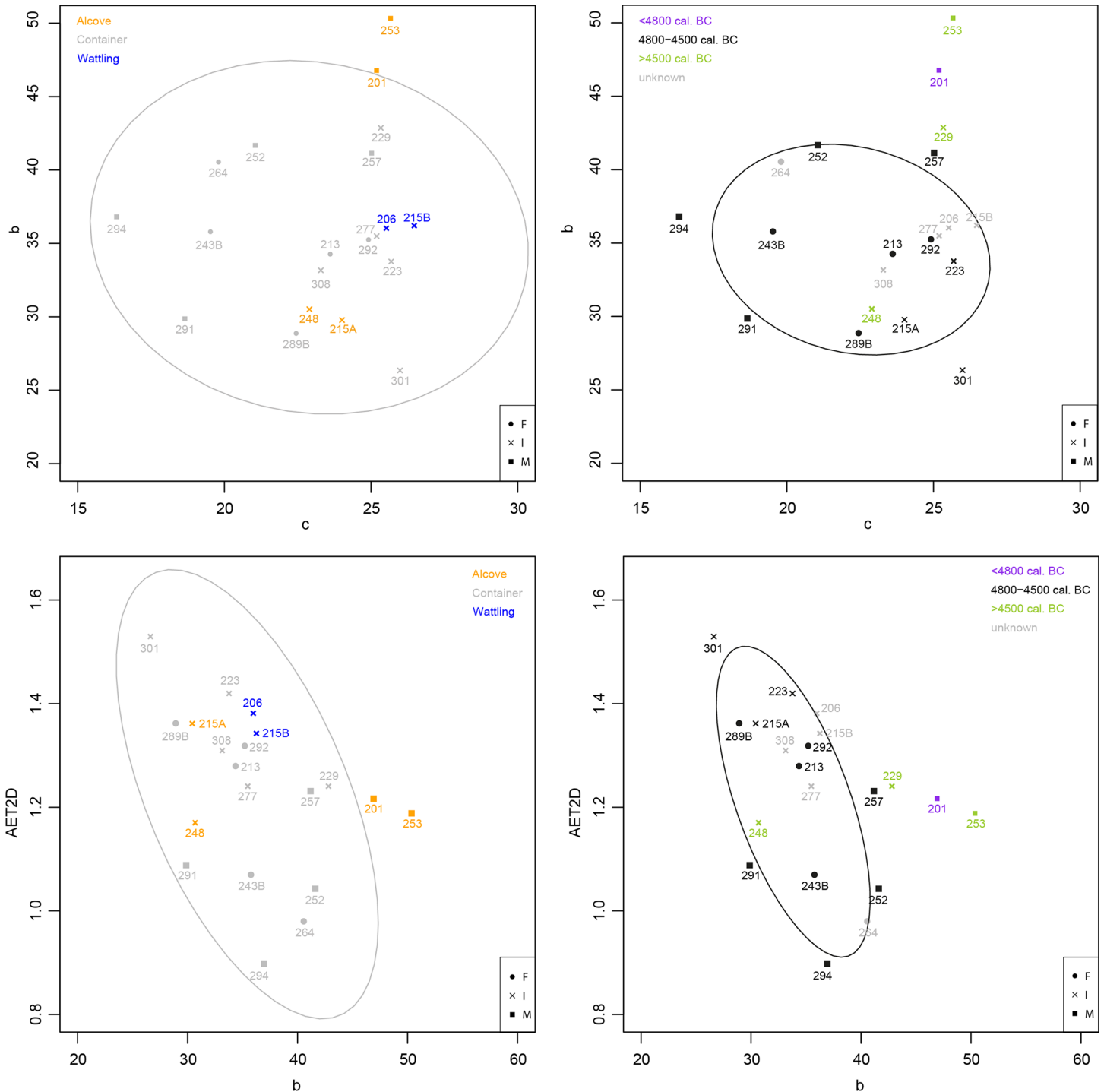
Fig 2. Plot of c against b (top) and plot of b against AET2D (graphic representation of RET2D, bottom) according to burial (left) and phase (right).

groups of individuals are found, especially considering final clusters. At the scale of the necropolis, the dendrogram clusters do not fit well into the spatial organization (see **S11 Fig**), suggesting that biological and spatial distances among individuals may not be strongly associated. However, at a smaller scale, the final clusters identified (**Fig 5**) are mostly supported by

Table 4. Measured 3D variables of crown tissue proportions for each individual.

Individual	Cvol	Evol	Dvol	DPvol	%DPvol	S_{EDJ}	AET3D	RET3D
201	565.30	268.09	281.42	297.21	52.58	201.57	1.33	19.93
206	410.86	209.73	168.26	201.13	48.95	159.34	1.32	22.47
213	383.43	199.18	182.83	184.25	48.05	150.36	1.32	23.28
215A	330.23	180.57	141.20	149.66	45.32	132.39	1.36	25.69
215B	401.50	208.45	179.16	193.05	48.08	158.93	1.31	22.69
223	442.63	234.91	141.24	207.72	46.93	161.83	1.45	24.51
229	478.58	240.55	237.69	238.03	49.74	184.39	1.30	21.05
243B	363.94	144.34	214.76	219.60	60.34	176.23	0.82	13.58
248	279.20	136.33	140.97	142.87	51.17	131.06	1.04	19.90
252	399.21	193.60	203.33	205.62	51.51	157.67	1.23	20.80
253	474.74	238.93	230.92	235.81	49.67	175.41	1.36	22.05
257	429.40	210.53	216.30	218.88	50.97	175.29	1.20	19.93
264	380.95	187.12	189.12	193.83	50.88	158.48	1.18	20.40
277	424.31	229.00	189.61	195.31	46.03	169.25	1.35	23.32
289B	370.49	214.24	150.01	156.25	42.17	138.42	1.55	28.74
291	314.69	127.33	186.40	187.35	59.54	145.39	0.88	15.31
292	428.73	230.34	196.17	198.39	46.27	162.34	1.42	24.33
294	383.65	149.97	228.08	233.68	60.91	176.03	0.85	13.83
301	424.02	250.02	171.59	174.00	41.04	153.83	1.63	29.11
308	375.34	212.61	161.17	162.73	43.36	140.57	1.51	27.70

Cvol = total crown volume (mm^3)

Evol = enamel volume (mm^3); DPvol = coronal dentin and pulp volume (mm^3)

%DPvol = percentage of crown that is dentin and pulp (%)

S_{EDJ} = enamel-dentin junction area (mm^2)

AET3D = 3D average enamel thickness (mm)

RET3D = 3D relative enamel thickness (scale free).

bootstrap higher than 90 (e.g., 229–253; 289B-308; 277–292; 243B-294). These subclusters include individuals who share multiple parameters, such as burial structure, orientation and

Table 5. Descriptive statistics of measured 3D variables for all individuals, female and male individuals, separately.

		Cvol	Evol	Dvol	DPvol	%DPvol	S_{EDJ}	AET3D	RET3D
All individuals	mean ± SD	403.06 ± 62.46	203.29 ± 39.22	190.51 ± 36.86	199.77 ± 35.87	49.83 ± 5.50	160.44 ± 18.07	1.27 ± 0.22	21.93 ± 4.34
	range	279.20–565.30	127.33–268.09	140.97–281.42	142.87–297.21	41.04–60.91	131.06–201.57	0.82–1.63	13.58–29.11
	CV	0.15	0.19	0.19	0.18	0.11	0.11	0.18	0.20
Female	mean ± SD	385.51 ± 25.42	195.04 ± 32.65	186.58 ± 23.69	190.46 ± 23.09	49.54 ± 6.81	157.17 ± 14.05	1.26 ± 0.28	22.06 ± 5.61
	range	363.94–428.73	144.34–230.34	150.01–214.76	156.25–219.60	42.17–60.34	138.42–176.23	0.82–1.55	13.58–28.74
	CV	0.07	0.17	0.13	0.12	0.14	0.09	0.22	0.25
Male	mean ± SD	427.83 ± 85.64	198.07 ± 53.04	224.41 ± 32.44	229.76 ± 37.69	54.19 ± 4.78	171.89 ± 19.11	1.14 ± 0.22	18.64 ± 3.28
	range	314.69–565.30	127.33–268.09	186.40–281.42	187.35–297.21	49.67–60.91	145.39–201.57	0.85–1.36	13.83–22.05
	CV	0.20	0.27	0.14	0.16	0.09	0.11	0.20	0.18

For the definitions of the abbreviated variables, see **Table 4**.
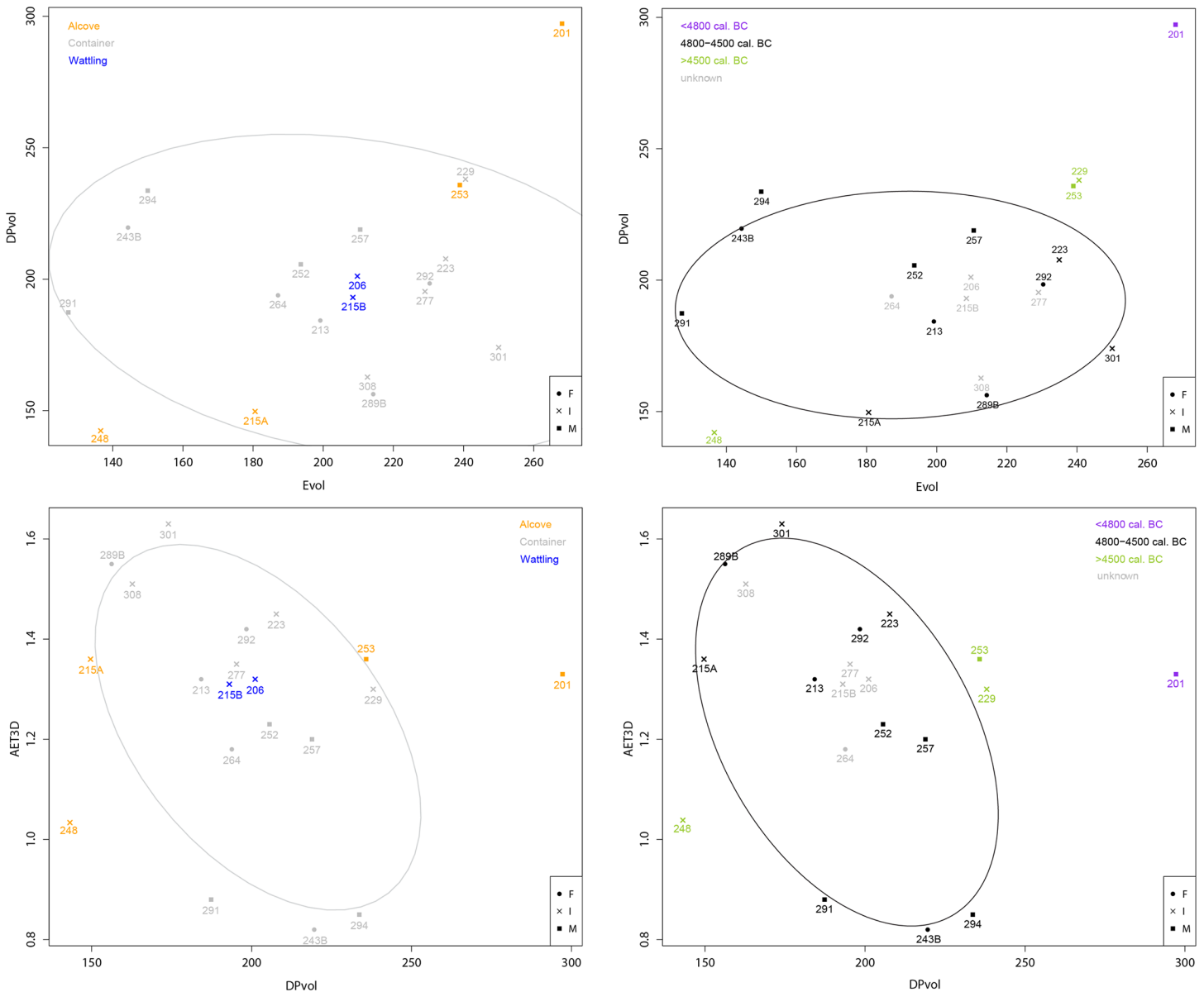
Fig 3. Plot of Evol against DPvol (top) and plot of DPvol against AET3D (graphic representation of RET3D, bottom) according to burial (left) and phase (right).

doi:10.1371/journal.pone.0159688.g003

location in the necropolis, position of the head and the body in the burial ([Table 1](#) and [S11 Fig](#)). Particularly, individuals 206-215B are spatially closed and both are buried in pit with wattling with the same orientation, even if the body of 206 is on the back and that of 215B on the left side, both have the head oriented to the south-east. Also, individuals 215A-248 share pits with alcove and are both buried on the left side with their head to the south.

EDJ shape

From geometric morphometric analysis, the first three principal components (PC) account for 30.12%, 15.86% and 13.91% of the total form variation of EDJ, respectively ([Fig 6](#)). PC1 mostly represents allometric size differences observed between males and females (correlation of PC1
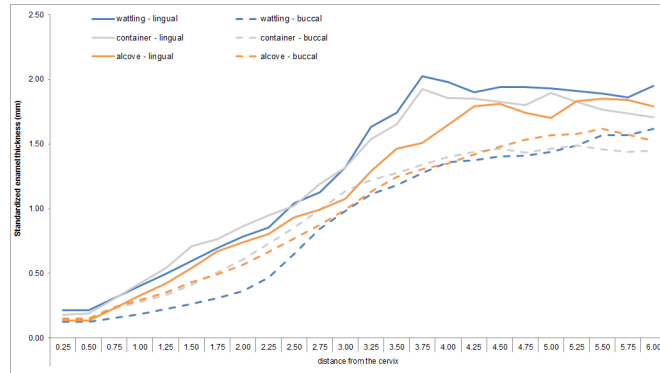
Fig 4. Topographic variation of standardized enamel thickness measured on the lingual (continuous lines) and buccal (dotted lines) aspects according to burial structures.

and lnCS: r = 0.975), while PC2 and PC3 allow visualization of only size-independent shape variations (correlations of PC2/PC3 and lnCS: r = 0.046 / r = 0.211. respectively). Minor sex differences in overall EDJ shape are observed, but males tend to have bigger EDJ, with higher dentin horn tips and buccolingual lengthening (S12 Fig).

Furthermore, individuals buried in a pit with wattling show an EDJ shape that is systematically included in the variability of those buried in pit with container (Fig 6). On the contrary, allometry particularly affects individuals buried in pit with alcove which are outside the variability observed for other individuals along PC1 (Fig 6). While males 201 and 253 possess the biggest EDJ and individuals 215A and 248 the smallest, these four individuals share a similar condition, illustrated by their position along PC3. Indeed, they present a reduction of the height of the distolingual dentin horn tip (hypocone) compared to the height of other horn tips.

Individuals from early (A) and recent (C) phases have EDJ shapes that fall at the extreme variation shown by the individuals from the principal phase (Fig 7). In particular, individual 201 from the early phase possesses an EDJ shape that sets him apart. As a whole, individuals from early and recent phases, and those buried in alcove seems to be distinguishable by their crown tissue proportions and EDJ shape, distinguishes them from the other individuals buried in the necropolis of Gurgy.

Discussion

In this study, crown tissue proportions, thickness and distribution of enamel, and EDJ shape have been used to explore phenotypic variations between the Neolithic individuals buried in the necropolis of Gurgy.

- Do phenotypic distances obtained from the study of morphological and metrical variation of internal tooth structure are a reliable proxy to track groups sharing similar chronocultural and burial practices?

While a relative homogeneity has been found in these variables, and particularly in enamel thickness topography, differences from internal tooth structure analysis could be correlated with burial and chronocultural parameters. Individuals buried in pits with alcove show subtle differences in their internal tooth structure from individuals found in pits with container and wattling. Moreover, individuals from early and recent phases of the necropolis could be distinguished from those of the principal phase from their crown tissue proportions and EDJ shape.
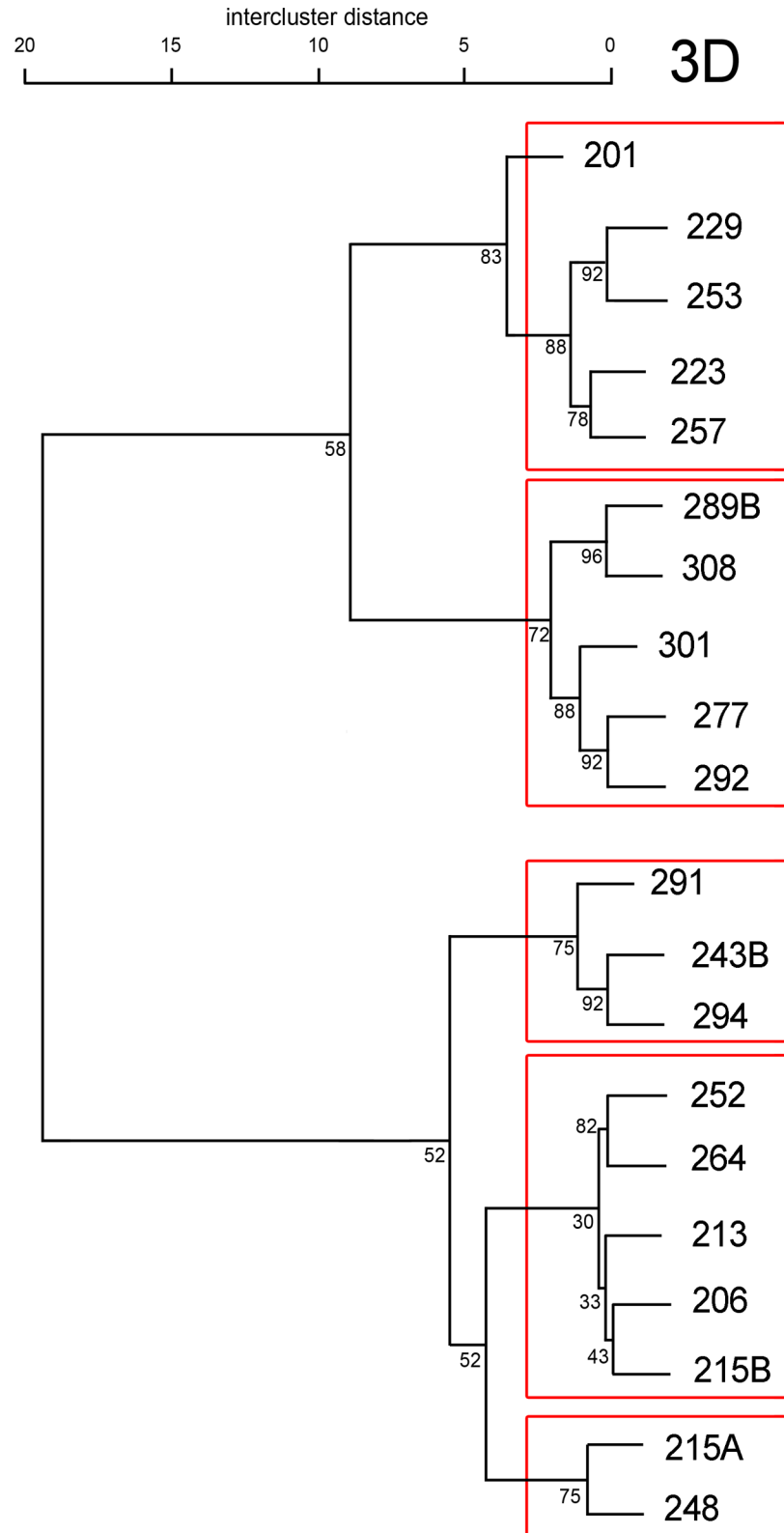
Fig 5. Dendrogram from cluster analysis based on 3D tissue proportions. Bootstrap values are indicated on nodes.
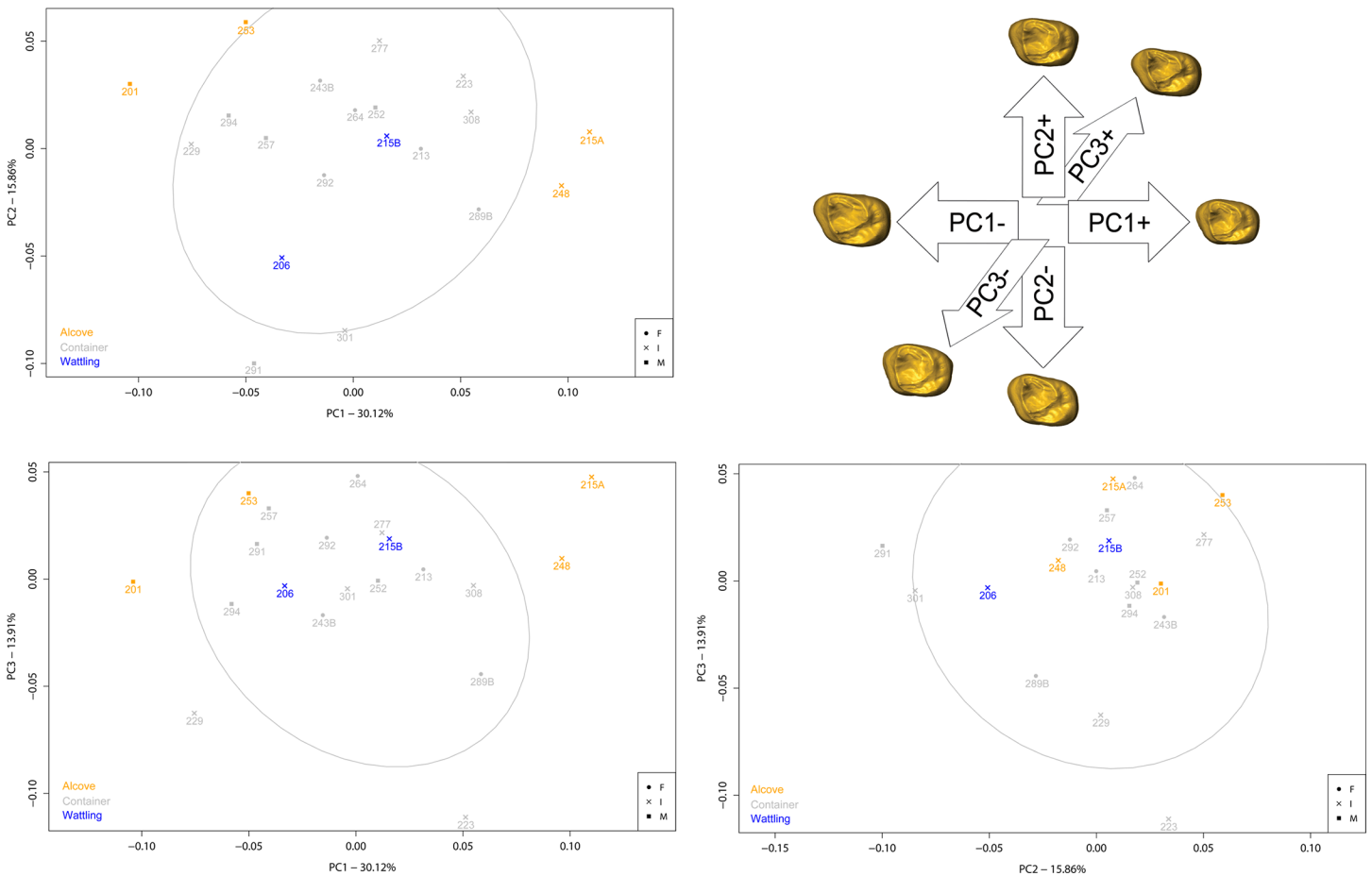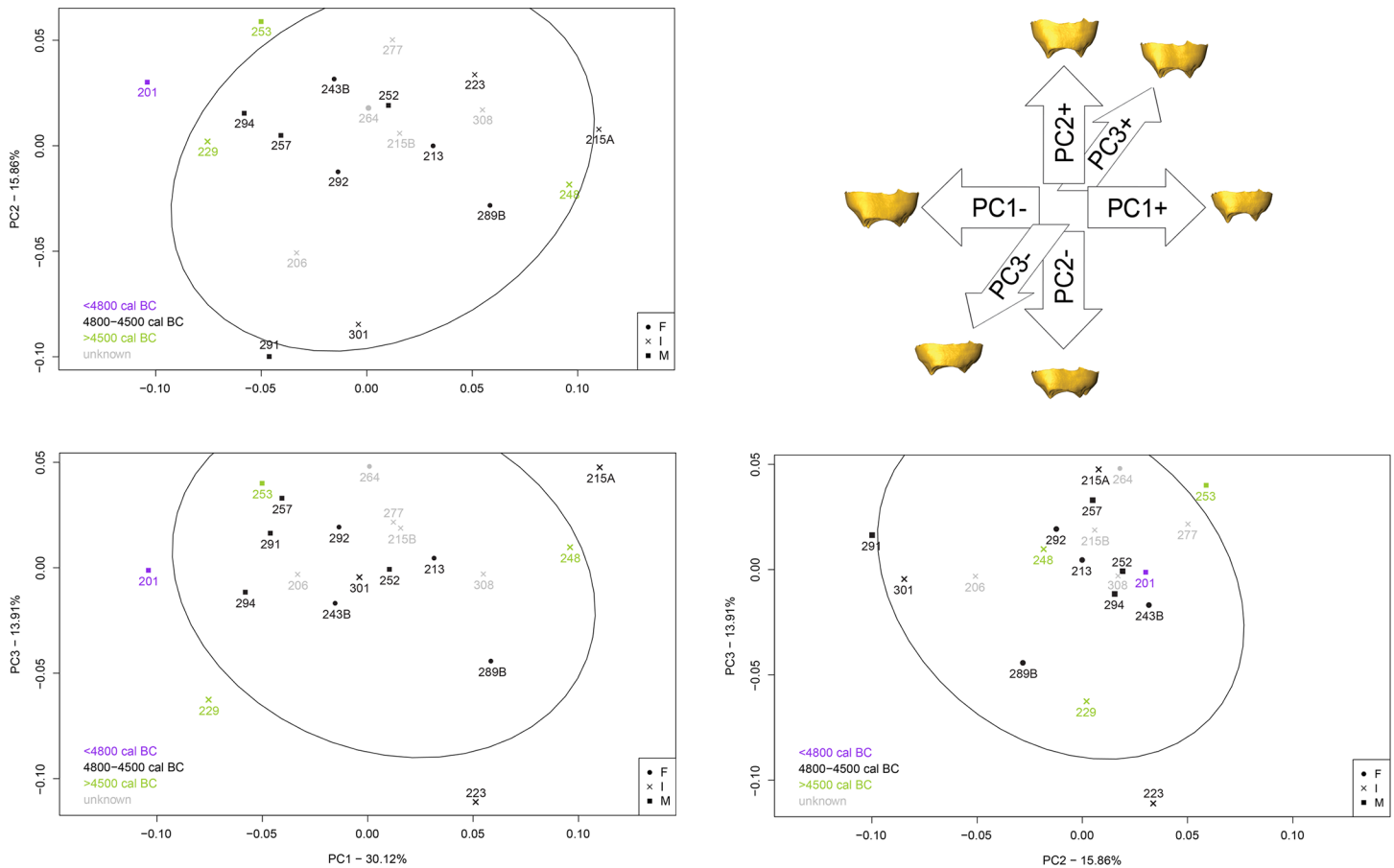
Fig 6. Result of PCA on the EDJ shape coordinates on form space, according to burial structures.

Moreover, it is noteworthy that pits with alcove are located at the south-west periphery of the necropolis area (see **Fig 1**). They were continuously used during the occupation of the necropolis, which started at the end of Early Neolithic period and ended during the Middle Neolithic period [112]. However, the only structure consisting of an alcove that is similar to those observed during the *Rubané Récent du Bassin Parisien (RRBP)* is the burial of individual 201 [150]. The RRBP is the latest expansion of the *Linearbandkeramik-derived* culture in Western Europe [151,152]. Moreover, paleogenetic data showed that both haplogroups inherited from hunter-gatherers and farmers are found in individuals buried in alcove [114]. The present data suggest that these individuals may have shared a cultural and phenotypical heritage from Early Neolithic. Also, despite the geographical location of the Neolithic necropolis of Gurgy at the confluence of the two waves of neolithization [111] and paleogenetic evidence of individuals derived from both waves [114], the funerary practices are relatively homogeneous at Gurgy [112], especially compared to the diversity that has been observed in the Paris Basin during Early/Middle Neolithic [115,153–156]. Moreover, data from isotopic analysis [117], enamel thickness topography and occlusal wear patterns [93] show an important homogeneity in the Neolithic population of Gurgy. In this context, the relative cultural and phenotypical distinctions of individuals buried in an alcove may more likely be in relation to inherited patterns from Ancient Neolithic groups.

Fig 7. Result of PCA on the EDJ shape coordinates on form space, according to occupation phases.

• Is one of these internal parameters more relevant to discuss interindividual variability?

Considering the subtle differences found at the intrasite scale, none of the internal parameters proved to be more relevant, it was the whole crown analysis that allowed to discuss differences linked to chronocultural variations and burial structures. However, the dentin component should be interpreted cautiously. In the necropolis of Gurgy, males have a greater quantity of crown tissues than females, but only the dentin volume differs significantly between sexes. Overall dimensions of the crown and dentin volume must be considered in the interpretation of the results. Also, the EDJs of males tend to be bigger than those of females, with higher dentin horn tips and buccolingual lengthening. These results are consistent with sexual dimorphism that has already been shown for internal crown structure, with men having higher enamel volume, dentin volume and EDJ area than women [109,110,157]. In this context, previous studies suggested that sexual dimorphism in external crown dimensions could be linked with a higher production of dentin in males compared to females [157–160].

• Can causes of dental variations be suggested?

While individuals buried in alcove show a size-related variation in internal crown proportions and morphology which differentiate males and females, both tend to share an identical size-independent EDJ shape trend. Indeed, it seems that the individuals buried in pits with alcove share a reduction in the height of their distolingual dentin horn tip, corresponding to

the hypocone. This functional cusp [161,162] which is the last to form during dental development [96,103,104] shows higher variability. This could be consistent with previous studies which showed that distal cusps are more plastic to environmental stress [163,164]. Besides, according to the patterning cascade model of cusp development [107], the location, size, and shape of the later-developing cusps are configured by the characteristics of the first-forming cusps [103]. This model predicts that small initial differences in cusp spacing will have cumulative effects on later-developing cusps during the morphogenetic process [107]. Also, while asymmetry of enamel thickness topography is systematically shown between the functional and the non-functional cusps of UM2 at Gurgy [93], the individuals in alcove share a slightly more homogenous pattern of enamel thickness distribution than that of the other individuals. While enamel thickness has been demonstrated to be an evolutionary plastic trait, selectively responsive to functionally-related dietary changes and wear [20,61,78,93,165], thick enamel has been shown to be a homoplastic trait [61]. Functionally-related adaptive changes of enamel have been demonstrated, notably enamel thickness is an evolutionary plastic trait selectively responsive to dietary changes, tooth fracture and occlusal wear [20,61,78,93,165]. Moreover, the distolingual cusp was expected to be the most sensitive to functional changes [93]. Thus, from the preliminary samples used in this study, differences at phenotypical and cultural levels are found for these Neolithic individuals. The balance between environmental, phylogenetic, developmental and functional aspects is hard to evaluate, and any of these aspects can be suggested as possible underlying cause for the origin of phenotypical differences shared by these individuals buried in alcove.

Conclusions

In this study of the Neolithic individuals from Gurgy, morphological and metric parameters such as crown tissue proportions, thickness and distribution of enamel, and EDJ shape, were assessed in a whole crown perspective, in order to finely quantify size and shape variations in a microevolutionary context. The results suggest that the internal tooth structure may be a reliable proxy to track groups sharing similar chronocultural and burial practices. Indeed, from the non-invasive characterization of their internal tooth structure, individuals buried in alcove have been distinguished from those buried in other structures, and underlying factors and causes of these dental variations have been discussed. The internal tooth structure could be used to discuss interindividual phenotypic variation within and between burial grounds, as well as to assess environmental, phylogenetic, developmental and/or functional underlying causes of these phenotypic variations. With adapted methods and templates designed to finely characterize variations at microevolutionary scales, further studies of teeth from osteological reference collections will elucidate to which extent these factors may be tracked in archeological samples.

Supporting Information

S1 Fig. Images of the three burial structures: pit with container (left), pit with wattling (middle), and pit with alcove (right).
(TIF)

S2 Fig. Multiple plot of radiocarbon ages available for the sampled individuals.
(TIF)

S3 Fig. Virtual buccolingual cross-section through the dentin horn tips of the mesial cusps of upper second molar, surface and linear variables (left), and standardized enamel thickness measured on the buccal aspect (right).
(TIF)

S4 Fig. 3D surface models of upper second molar (a); dental tissues in transparence (b) (enamel in white, dentin in yellow, pulp in orange) with position of the cervical plane for virtual isolation of the crown; and resulting measured volumes: total crown volume (c), enamel volume (d), coronal dentin volume (e).
(TIF)

S5 Fig. EDJ template. Landmarks are represented in black spheres, curve semilandmarks in grey spheres, and surface semilandmarks in white spheres.
(TIF)

S6 Fig. Plot of c against b (left) and plot of b against AET2D (right) according to the sex of individuals.
(TIF)

S7 Fig. Comparative morphology of each UM2 crown. Reconstructions of outer enamel surface (OES), enamel-dentin junction (EDJ), dental tissue proportions (DTP) with superposition of enamel and dentin in transparence, and cartography of enamel thickness (ET) in occlusal (O), mesial (M), distal (D), buccal (B) and lingual (L) views.
(PDF)

S8 Fig. Plot of Evol against DPvol (left) and plot of DPvol against AET3D (right) according to the sex of individuals.
(TIF)

S9 Fig. Dendrogram from cluster analysis based on 2D tissue proportions. Bootstrap values are indicated on nodes.
(TIF)

S10 Fig. Cluster analysis performed on enamel component only (Evol and c, left) and dentin component only (DPvol and b, right).
(TIF)

S11 Fig. Necropolis map of Gurgy with details of cultural parameters for individuals clustered according to the dendrogram obtained from 3D tissue proportions.
(TIF)

S12 Fig. ACP on EDJ according to the sex of individuals.
(TIF)

Acknowledgments

Author Contributions

Conceived and designed the experiments: MLL MC SR PB. Performed the experiments: MLL PB. Analyzed the data: MLL MC SR PB. Contributed reagents/materials/analysis tools: MLL MC SR PB. Wrote the paper: MLL MC SR PB.

References

1. Hanihara K. Criteria for classification of crown characters of the human deciduous dentition. J Anthrop Soc Nippon 1961; 69: 27–45.

2. Hanihara K. Mongoloid dental complex in the deciduous dentition. J Anthrop Soc Nippon 1966; 74: 61–72.

3. Garn SM, Lewis AB, Walenga AJ. Crown-size profile patterns and presumed evolutionary "trends". Am Anthropol 1969; 71: 79–84.

4. Alvesalo L, Tigerstedt PMA. Heritabilities of human tooth dimensions. Hereditas 1974; 77: 311–318. PMID: 4448690

5. Townsend G, Brown T. Heritability of permanent tooth size. Am J Phys Anthropol 1978; 49: 497–504. PMID: 736106

6. Townsend G. Heritability of deciduous tooth size in Australian Aboriginals. Am J Phys Anthropol 1980; 53: 297–300. PMID: 7416257

7. Scott GR, Turner CG. The anthropology of modern human teeth. Dental morphology and its variation in recent human populations. Cambridge: Cambridge University Press; 1997.

8. Irish JD. Population continuity vs. discontinuity revisited: dental affinities among late Paleolithic through Christian-era Nubians. Am J Phys Anthropol 2005; 128: 520–535. PMID: 15895433

9. Irish JD. Who were the ancient Egyptians? Dental affinities among Neolithic through postdynastic peoples. Am J Phys Anthropol 2006; 129: 529–543. PMID: 16331657

10. Hanihara T, Ishida H. Metric dental variation of major human populations. Am J Phys Anthropol 2005; 128: 287–298. PMID: 15838862

11. Hanihara T. Morphological variation of major human populations based on nonmetric dental traits. Am J Phys Anthropol 2008; 136: 169–182. doi: 10.1002/ajpa.20792 PMID: 18257017

12. Brook AH, Griffin RC, Townsend G, Levisianos Y, Russell J, Smith RN. Variability and patterning in permanent tooth size of four human ethnic groups. Arch Oral Biol 2009; 54 Suppl 1: S79–85. doi: 10.1016/j.archoralbio.2008.12.003 PMID: 19144325

13. Lukacs JR, Pal JN. Dental morphology of early Holocene foragers of North India: non-metric trait frequencies and biological affinities. HOMO 2013; 64: 411–436. doi: 10.1016/j.jchb.2013.08.003 PMID: 24050393

14. Kenyhercz MW, Klales AR, Kenyhercz WE. Molar size and shape in the estimation of biological ancestry: A comparison of relative cusp location using geometric morphometrics and interlandmark distances. Am J Phys Anthropol 2014; 153: 269–279. doi: 10.1002/ajpa.22429 PMID: 24248428

15. Paul KS, Stojanowski CM. Performance analysis of deciduous morphology for detecting biological siblings. Am J Phys Anthropol 2015; 157: 615–629. doi: 10.1002/ajpa.22755 PMID: 25921791

16. Hughes TE, Townsend GC. Twin and family studies of human dental crown morphology: genetic, epigenetic, and environmental determinants of the modern human dentition. In: Scott GR, Irish JD, editors. Anthropological perspectives on tooth morphology: genetics, evolution, variation. Cambridge: Cambridge University Press; 2013. pp. 31–68.

17. Townsend G, Bockmann M, Hughes T, Brook A. Genetic, environmental and epigenetic influences on variation in human tooth number, size and shape. Odontology / the Society of the Nippon Dental University 2012; 100: 1–9. doi: 10.1007/s10266-011-0052-z PMID: 22139304

18. Dempsey PJ, Townsend G. Genetic and environmental contributions to variation in human tooth size. Heredity 2001; 86: 685–693. PMID: 11595049

19. Townsend G, Hughes T, Luciano M, Bockmann M, Brook A. Genetic and environmental influences on human dental variation: a critical evaluation of studies involving twins. Arch Oral Biol 2009; 54 Suppl 1: S45–51. doi: 10.1016/j.archoralbio.2008.06.009 PMID: 18715551

20. Hlusko LJ, Suwa G, Kono RT, Mahaney MC. Genetics and the evolution of primate enamel thickness: a baboon model. Am J Phys Anthropol 2004; 124: 223–233. PMID: 15197818

21. Hlusko LJ. Elucidating the evolution of hominid dentition in the age of phenomics, modularity, and quantitative genetics. Annals of Anatomy 2016; 203: 3–11. doi: 10.1016/j.aanat.2015.05.001 PMID: 26100767

22. Corruccini RS, Sharma K, Potter RH. Comparative genetic variance and heritability of dental occlusal variable in U.S. and northwest indian twins. Am J Phys Anthropol 1986; 70: 293–299. PMID: 3752227

23. Eguchi S, Townsend GC, Richards LC, Hughes T, Kasai K. Genetic contribution to dental arch size variation in Australian twins. Arch Oral Biol 2004; 49: 1015–1024. PMID: 15485644

24. Hughes CE, Thomas C, Richards L, Townsend G. A study of occlusal variation in the primary dentition of Australian twins and singletons. Arch Oral Biol 2001; 46: 857–864. PMID: 11420058

25. Potter RH, Corruccini RS, Green LJ. Variance of occlusion traits in twins. J Craniofac Genet Dev Biol 1981; 1: 217–227. PMID: 7200099

26. Calcagno JM. Dental reduction in Post-Pleistocene Nubia. Am J Phys Anthropol 1986; 70: 349–363. PMID: 3092673

27. Potter RH, Nance WE. A twin study of dental dimension. I. Discordance, asymmetry, and mirror imagery. Am J Phys Anthropol 1976; 44: 391–396. PMID: 945700

28. Potter RH, Nance WE, Yu P-L, Davis WB. A twin study of dental dimension. II. Independant genetic determinants. Am J Phys Anthropol 1976; 44: 397–412. PMID: 945701

29. Berry AC, Berry RJ. Epigenetic variation in the human cranium. J Anat 1967; 101: 361–379. PMID: 4227311

30. Hauser G, De Stefano GF. Epigenetic variants of the human skull. Stuttgart: E. Schweizerbart'sche Verlagsbuchhandlung; 1989.

31. Crubezy É, Sellier P. Caractères discrets et « recrutement » des ensembles sépulcraux. Bull Mém Soc Anthropol Paris 1990; 2: 171–177.

32. Turner CG. Late Pleistocene and Holocene population history of East Asia based on dental variation. Am J Phys Anthropol 1987; 73: 305–321. PMID: 3303958

33. Crubezy É, Sellier P. Liens de parenté et populations inhumées. Les nouvelles de l'archéologie 1990; 40: 35–37.

34. Irish JD. Ancestral dental traits in recent Sub-Saharan Africans and the origins of modern humans. J Hum Evol 1997; 34: 81–98.

35. Gemmerich Pfister IG. Création d'une collection anthropologique de référence et application des caractères discrets dans le cas de généalogies connues. Thèse de doctorat, Université de Genève. 1999.

36. Desideri J. Les traits non métriques dentaires sont-ils de bons indicateurs des distances biologiques entre les populations? In: Besse M, Stahl G, Laurence I, Curdy P, editors. ConstellaSion. Hommage à Alain Gallay. Lausanne: Cahiers d'archéologie romande; 2003. pp. 447–462.

37. Matsumura H, Hudson MJ. Dental perspectives on the population history of Southeast Asia. Am J Phys Anthropol 2005; 127: 182–209. PMID: 15558609

38. Ullinger JM, Sheridan SG, Hawkey DE, Turner CG, 2nd, Cooley R. Bioarchaeological analysis of cultural transition in the southern Levant using dental nonmetric traits. Am J Phys Anthropol 2005; 128: 466–476. PMID: 15895418

39. Irish JD, Guatelli-Steinberg D, Legge SS, de Ruiter DJ, Berger LR. Dental morphology and the phylogenetic "place" of Australopithecus sediba. Science 2013; 340: 1233062. doi: 10.1126/science.1233062 PMID: 23580535

40. Irish JD, Guatelli-Steinberg D, Legge SS, de Ruiter DJ, Berger LR. News and views: response to 'Non-metric dental traits and hominin phylogeny' by Carter et al., with additional information on the Arizona State University Dental Anthropology System and phylogenetic 'place' of Australopithecus sediba. J Hum Evol 2014; 69: 129–134. doi: 10.1016/j.jhevol.2014.01.004 PMID: 24529864

41. Irish JD. Questions of khoesan continuity: dental affinities among the indigenous Holocene peoples of South Africa. Am J Phys Anthropol 2014; 155: 33–44. doi: 10.1002/ajpa.22526 PMID: 24789680

42. Coppa A, Cucina A, Lucci M, Mancinelli D, Vargiu R. Origins and spread of agriculture in Italy: a nonmetric dental analysis. Am J Phys Anthropol 2007; 133: 918–930. PMID: 17455286

43. Delgado-Burbano ME. Population affinities of African Colombians to Sub-Saharan Africans based on dental morphology. HOMO 2007; 58: 329–356. PMID: 17675007

44. Thomas A. Identités funéraires, variants biologiques et facteurs chronologiques: une nouvelle perception du contexte culturel et social du Cerny (Bassin parisien, 4700–4300 avant J.-C.). Thèse de doctorat, Université Bordeaux 1. 2011.

45. Zubova AV. Non-metric dental trait variation among Eastern European and Western Siberian forest-steppe Neolithic populations. Bull Int Assoc Paleodont 2014; 8: 244–257.

46. McIlvaine BK, Schepartz LA, Larsen CS, Sciulli PW. Evidence for long-term migration on the Balkan Peninsula using dental and cranial nonmetric data: Early interaction between Corinth (Greece) and its colony at Apollonia (Albania). Am J Phys Anthropol 2014; 153: 236–248. doi: 10.1002/ajpa.22425 PMID: 24227263

47. Crubezy É, Telmon N, Sevin A, Picard J, Rougé D, Larrouy G, et al. Microévolution d'une population historique. Étude des caractères discrets de la population de Missiminia (Soudan, IIIe-VIe siècle). Bull Mém Soc Anthropol Paris 1999; 11: 1–213.

48. Sansilbano-Collilieux M. Les caractères discrets et le recrutement de deux nécropoles du Haut Moyen Age à Poitiers (Vienne). Bull Mém Soc Anthropol Paris 1990; 2: 179–183.

49. Stojanowski CM, Schillaci MA. Phenotypic approaches for understanding patterns of intracemetery biological variation. Am J Phys Anthropol 2006; Suppl 43: : 49–88. PMID: 17103428

50. Bondioli L, Corruccini RS, Macchiarelli R. Familial segregation in the Iron Age community of Alfedena, Abruzzo, Italy, based on osteodental trait analysis. Am J Phys Anthropol 1986; 71: 393–400. PMID: 3812655

51. Johnson AL, Lovell NC. Biological differentiation at Predynastic Naqada, Egypt: an analysis of dental morphological traits. Am J Phys Anthropol 1994; 93: 427–433. PMID: 8048465

52. Laforest C, Castex D, Cartron I, Murail P. Microévolution d'une population historique sur les rives de l'estuaire de la Gironde. Bull Mém Soc Anthropol Paris 2011; 24: 12–24.

53. Keyser-Traqui C, Crubézy E, Ludes B. Nuclear and mitochondrial analysis of a 2000-year-old necropolis in the Egyin Gol valley of Mongolia. Am J Hum Genet 2003; 73: 247–260. PMID: 12858290

54. Haak W, Brandt G, de Jong HN, Meyer C, Ganslmeier R, Heyd V, et al. Ancient DNA, strontium isotopes, and osteological analyses shed light on social and kinship organization of the Later Stone Age. Proc Natl Acad Sci U S A 2008; 105: 18226–18231. doi: 10.1073/pnas.0807592105 PMID: 19015520

55. Deguilloux M- F, Pemonge M- H, Mendisco F, Thibon D, Cartron I, Castex D. Ancient DNA and kinship analysis of human remains deposited in Merovingian necropolis sarcophagi (Jau Dignac et Loirac, France, 7th-8th century AD). J Anthropol Sci 2014; 41: 399–405.

56. Bentley RA, Bickle P, Fibiger L, Nowell GM, Dale CD, Hedges REM, et al. Community differenciation and kinship among Europe's first farmers. Proc Natl Acad Sci U S A 2012; 109: 9326–9330. doi: 10.1073/pnas.1113710109 PMID: 22645332

57. Ricaut FX, Auriol V, von Cramon-Taubadel N, Keyser C, Murail P, Ludes B, et al. Comparison between morphological and genetic data to estimate biological relationship: the case of the Egyin Gol necropolis (Mongolia). Am J Phys Anthropol 2010; 143: 355–364. doi: 10.1002/ajpa.21322 PMID: 20949608

58. Herrera B, Hanihara T, Godde K. Comparability of multiple data types from the Bering strait region: cranial and dental metrics and nonmetrics, mtDNA, and Y-chromosome DNA. Am J Phys Anthropol 2014; 154: 334–348. doi: 10.1002/ajpa.22513 PMID: 24643445

59. Hubbard AR, Guatelli-Steinberg D, Irish JD. Do nuclear DNA and dental nonmetric data produce similar reconstructions of regional population history? An example from modern coastal Kenya. Am J Phys Anthropol 2015; 157: 295–304. doi: 10.1002/ajpa.22714 PMID: 25711463

60. Dean MC. Tooth microstructure tracks the pace of human life-history evolution. Proc Biol Sci 2006; 273: 2799–2808. PMID: 17015331

61. Pampush JD, Duque AC, Burrows BR, Daegling DJ, Kenney WF, McGraw WS. Homoplasy and thick enamel in primates. J Hum Evol 2013; 64: 216–224. doi: 10.1016/j.jhevol.2013.01.009 PMID: 23415414

62. Macchiarelli R, Bondioli L, Débénath A, Mazurier A, Tournepiche J- F, Birch W, et al. How Neanderthal molar teeth grew. Nature 2006; 444: 748–751. PMID: 17122777

63. Macchiarelli R, Bayle P, Bondioli L, Mazurier A, Zanolli C. From outer to inner structural morphology in dental anthropology. The integration of the third dimension in the vizualisation and quantitative analysis of fossil remains. In: Scott RG, Irish JD, editors. Anthropological perspectives on tooth morphology: genetics, evolution, variation. Cambridge: Cambridge University Press; 2013. pp. 250–277.

64. Macchiarelli R, Bondioli L, Mazurier A. Virtual dentitions: touching the hidden evidence. In: Irish JD, Nelson GC, editors. Technique and application in dental anthropology. Cambridge: Cambridge University Press; 2008. pp. 426–448.

65. Skinner MF. Enamel-dentine junction morphology of extant hominoid and fossil hominin lower molars. PhD dissertation, George Washington University. 2008.

66. Skinner MM, Alemseged Z, Gaunitz C, Hublin JJ. Enamel thickness trends in Plio-Pleistocene hominin mandibular molars. J Hum Evol 2015; 85: 35–45. doi: 10.1016/j.jhevol.2015.03.012 PMID: 26024565

67. Smith TM. Teeth and human life-history evolution. A Rev Anthropol 2013; 42: 191–208.

68. Smith TM, Olejniczak AJ, Reh S, Reid DJ, Hublin JJ. Brief communication: enamel thickness trends in the dental arcade of humans and chimpanzees. Am J Phys Anthropol 2008; 136: 237–241. doi: 10.1002/ajpa.20796 PMID: 18324634

69. Smith TM, Olejniczak AJ, Zermeno JP, Tafforeau P, Skinner MM, Hoffmann A, et al. Variation in enamel thickness within the genus *Homo*. J Hum Evol 2012; 62: 395–411. doi: 10.1016/j.jhevol.2011.12.004 PMID: 22361504

70. Smith TM, Tafforeau P, Le Cabec A, Bonnin A, Houssaye A, Pouech J, et al. Dental ontogeny in Plio-cene and Early Pleistocene hominins. PLOS ONE 2015; 10: e0118118. doi: 10.1371/journal.pone. 0118118 PMID: 25692765

71. Guatelli-Steinberg D. Recent studies of dental development in Neandertals: Implications for Neander-tal life histories. Evolutionary Anthropology: Issues, News, and Reviews 2009; 18: 9–20.

72. Guatelli-Steinberg D, Reid DJ, Bishop TA. Did the lateral enamel of Neandertal anterior teeth grow dif-ferently from that of modern humans? J Hum Evol 2007; 52: 72–84. PMID: 16965802

73. Bondioli L, Bayle P, Dean MC, Mazurier A, Puymerail L, Ruff CB, et al. Technical note: morphometric maps of long bone shafts and dental roots for imaging topographic thickness variation. Am J Phys Anthropol 2010; 142: 328–334. doi: 10.1002/ajpa.21271 PMID: 20229503

74. Bailey SE, Skinner MM, Hublin J- J. What lies beneath? An evaluation of lower molar trigonid crest patterns based on both dentine and enamel expression. Am J Phys Anthropol 2011; 145: 505–518. doi: 10.1002/ajpa.21468 PMID: 21312178

75. Kupczik K, Hublin JJ. Mandibular molar root morphology in Neanderthals and Late Pleistocene and recent *Homo sapiens*. J Hum Evol 2010; 59: 525–541. doi: 10.1016/j.jhevol.2010.05.009 PMID: 20719359

76. Dean MC, Cole T. The timing of our tooth growth is an evolutionary relic. Significance 2014; 11: 19–23.

77. Crevecoeur I, Skinner MM, Bailey SE, Gunz P, Bortoluzzi S, Brooks AS, et al. First early hominin from Central Africa (Ishango, Democratic Republic of Congo). PLOS ONE 2014; 9: e84652. doi: 10.1371/journal.pone.0084652 PMID: 24427292

78. Horvath JE, Ramachandran GL, Fedrigo O, Nielsen WJ, Babbitt CC, St Clair EM, et al. Genetic com-parisons yield insight into the evolution of enamel thickness during human evolution. J Hum Evol 2014; 73: 75–87. doi: 10.1016/j.jhevol.2014.01.005 PMID: 24810709

79. Braga J, Thackeray JF, Subsol G, Kahn JL, Maret D, Treil J, et al. The enamel-dentine junction in the postcanine dentition of *Australopithecus africanus*: intra-individual metameric and antimeric variation. J Anat 2010; 216: 62–79. doi: 10.1111/j.1469-7580.2009.01154.x PMID: 19900182

80. Schwartz GT, Dean MC. Charting the chronology of developing dentitions. In: Irish JD, Nelson GC, editors. Technique and application in dental anthropology. Cambridge: Cambridge University Press; 2008. pp. 219–233.

81. Martin L. Significance of enamel thickness in hominoid evolution. Nature 1985; 314: 260–263. PMID: 3920525

82. Macho GA, Berner M. Enamel thickness of human maxillary molars reconsidered. Am J Phys Anthro-pol 1993; 92: 189–200. PMID: 8273831

83. Kono RT, Suwa G, Tanijiri T. A three-dimensional analysis of enamel distribution patterns in human permanent first molars. Arch Oral Biol 2002; 47: 867–875. PMID: 12450518

84. Kono RT. Molar enamel thickness and distribution patterns in extant great apes and humans: new insights based on a 3-dimensional whole crown perspective. Anthropol Sci 2004; 112: 121–146.

85. Olejniczak AJ, Tafforeau P, Feeney RN, Martin LB. Three-dimensional primate molar enamel thick-ness. J Hum Evol 2008; 54: 187–195. PMID: 18045652

86. Olejniczak AJ, Smith TM, Feeney RN, Macchiarelli R, Mazurier A, Bondioli L, et al. Dental tissue pro-portions and enamel thickness in Neandertal and modern human molars. J Hum Evol 2008; 55: 12–23. doi: 10.1016/j.jhevol.2007.11.004 PMID: 18321561

87. Olejniczak AJ, Smith TM, Skinner MM, Grine FE, Feeney RN, Thackeray JF, et al. Three-dimensional molar enamel distribution and thickness in *Australopithecus* and *Paranthropus*. Biol Lett 2008; 4: 406–410. doi: 10.1098/rsbl.2008.0223 PMID: 18522924

88. Bayle P, Braga J, Mazurier A, Macchiarelli R. Dental developmental pattern of the Neanderthal child from Roc de Marsal: a high-resolution 3D analysis. J Hum Evol 2009; 56: 66–75. doi: 10.1016/j.jhevol.2008.09.002 PMID: 18986680

89. Bayle P, Macchiarelli R, Trinkaus E, Duarte C, Mazurier A, Zilhão J. Dental maturational sequence and dental tissue proportions in the early Upper Paleolithic child from Abrigo do Lagar Velho, Portugal. Proc Natl Acad Sci U S A 2010; 107: 1338–1342. doi: 10.1073/pnas.0914202107 PMID: 20080622

90. Suwa G, Kono RT, Simpson SW, Asfaw B, Lovejoy CO, White TD. Paleobiological implications of the *Ardipithecus ramidus* dentition. Science 2009; 326: 94–99. PMID: 19810195

91. Skinner MM, Gunz P, Wood BA, Hublin JJ. Enamel-dentine junction (EDJ) morphology distinguishes the lower molars of *Australopithecus africanus* and *Paranthropus robustus*. J Hum Evol 2008; 55: 979–988. doi: 10.1016/j.jhevol.2008.08.013 PMID: 18824253

92. Skinner MM, Evans A, Smith T, Jernvall J, Tafforeau P, Kupczik K, et al. Brief communication: contributions of enamel-dentine junction shape and enamel deposition to primate molar crown complexity. Am J Phys Anthropol 2010; 142: 157–163. doi: 10.1002/ajpa.21248 PMID: 20091839

93. Le Luyer M, Rottier S, Bayle P. Brief communication: comparative patterns of enamel thickness topography and oblique molar wear in two Early Neolithic and medieval population samples. Am J Phys Anthropol 2014; 155: 162–172. doi: 10.1002/ajpa.22562 PMID: 24961878

94. Zanolli C, Bayle P, Macchiarelli R. Tissue proportions and enamel thickness distribution in the early Middle Pleistocene human deciduous molars from Tighenif, Algeria. CR Palevol 2010; 9: 341–348.

95. Zanolli C, Grine FE, Kullmer O, Schrenk F, Macchiarelli R. The early Pleistocene deciduous hominid molar FS-72 from the Sangiran Dome of Java, Indonesia: a taxonomic reappraisal based on its comparative endostructural characterization. Am J Phys Anthropol 2015; 157: 666–674. doi: 10.1002/ajpa.22748 PMID: 25845703

96. Butler PM. The ontogeny of molar pattern. Biological Reviews 1956; 31: 30–69.

97. Morita W, Yano W, Nagaoka T, Abe M, Ohshima H, Nakatsukasa M. Patterns of morphological variation in enamel-dentin junction and outer enamel surface of human molars. J Anat 2014; 224: 669–680. doi: 10.1111/joa.12180 PMID: 24689536

98. Guy F, Lazzari V, Gilissen E, Thiery G. To what extent is primate second molar enamel occlusal morphology shaped by the enamel-dentine junction? PLOS ONE 2015; 10: e0138802. doi: 10.1371/journal.pone.0138802 PMID: 26406597

99. Smith TM, Olejniczak AJ, Reid DJ, Ferrell RJ, Hublin JJ. Modern human molar enamel thickness and enamel-dentine junction shape. Arch Oral Biol 2006; 51: 974–995. PMID: 16814245

100. Olejniczak AJ, Gilbert CC, Martin LB, Smith TM, Ulhaas L, Grine FE. Morphology of the enamel-dentine junction in sections of anthropoid primate maxillary molars. J Hum Evol 2007; 53: 292–301. PMID: 17582465

101. Skinner MM, Wood BA, Boesch C, Olejniczak AJ, Rosas A, Smith TM, et al. Dental trait expression at the enamel-dentine junction of lower molars in extant and fossil hominoids. J Hum Evol 2008; 54: 173–186. PMID: 18048081

102. Korenhof CAW. The enamel-dentine border: a new morphological factor in the study of the (human) molar pattern. Proceeding of the Kononklijke Nederlandse Akademie van Wetenschappen—Amsterdam; 1961. pp. 639–664.

103. Salazar-Ciudad I, Jernvall J. A gene network model accounting for development and evolution of mammalian teeth. Proc Natl Acad Sci U S A 2002; 99: 8116–8120. PMID: 12048258

104. Skinner MM, Gunz P. The presence of accessory cusps in chimpanzee lower molars is consistent with a patterning cascade model of development. J Anat 2010; 217: 245–253. doi: 10.1111/j.1469-7580.2010.01265.x PMID: 20629983

105. Guatelli-Steinberg D, Hunter JP, Durner RM, Moormann S, Weston TCB, Tracy K. Teeth, morphogenesis, and levels of variation in the human Carabelli trait. In: Scott GR, Irish JD, editors. Anthropological perspectives on tooth morphology: genetics, evolution, variation. Cambridge: Cambridge University Press; 2013. pp. 69–91.

106. Hunter JP, Guatelli-Steinberg D, Weston TC, Durner RM, Betsinger TK. Model of tooth morphogenesis predicts carabelli cusp expression, size, and symmetry in humans. PLOS ONE 2010; 5: e11844. doi: 10.1371/journal.pone.0011844 PMID: 20689576

107. Jernvall J, Jung H- S. Genotype, phenotype and developmental biology of molar tooth characters. Yearbook of Physical Anthropology 2000; 43: 171–190.

108. Evans AR, Daly ES, Catlett KK, Paul KS, King SJ, Skinner MM, et al. A simple rule governs the evolution and development of hominin tooth size. Nature 2016; 530: 477–480. doi: 10.1038/nature16972 PMID: 26911784

109. Feeney RN, Olejniczak A, Hublin J-J. Three-dimensional microtomographic analysis of sexual dimorphism in human molar-crown tissues. Am J Phys Anthropol 2010; S50: 103.

110. Feeney RNM, Zermeno JP, Reid DJ, Nakashima S, Sano H, Bahar A, et al. Enamel thickness in Asian human canines and premolars. Anthropol Sci 2010; 118: 191–198.

111. Rottier S, Mordant C, Chambon P, Thevenet C. Découverte de plus d'une centaine de sépultures du Néolithique moyen à Gurgy, les Noisats (Yonne). Bull Soc Préhist Fr 2005; 102: 641–645.

112. Rottier S. L'architecture funéraire des sépultures du Néolithique moyen des Noisats à Gurgy (Yonne, France). In: Moinat P, Chambon P, editors. Les cistes de Chamblandes et la place des coffres dans les pratiques funéraires du Néolithique moyen occidental. Actes du colloque de Lausanne, 12–13 mai 2006: Cahiers d'archéologie romande; 2007. pp. 99–107.

113. Le Roy M. Les enfants au Néolithique: du contexte funéraire à l'interprétation socioculturelle en France de 5700 à 2100 ans avant J.-C. Thèse de doctorat, Université de Bordeaux. 2015.

114. Rivollat M, Mendisco F, Pemonge M-H, Safi A, Saint-Marc D, Bremond A, et al. When the waves of European neolithization met: first paleogenetic evidence from early farmers in the southern Paris Basin. PLOS ONE 2015; 10: e0125521. doi: 10.1371/journal.pone.0125521 PMID: 25928633

115. Chambon P, Rottier S, Augereau A, Bonnardin S, Meunier K, Pariat J-G, et al. Évolution, coexistence et confrontation de pratiques funéraires entre 4700 et 4000 av. J.-C. sur un microterritoire dans la vallée de l'Yonne. In: Jaubert J, Fourment N, Depaepe P, editors. Transitions, ruptures et continuité en Préhistoire. Volume 1: Évolution des techniques, comportements funéraires, Néolithique ancien. XXVIIe congrès préhistorique de France, Bordeaux—Les Eyzies, 31 mai—5 juin 2010: Société Préhistorique Française; 2013. pp. 213–228.

116. Le Roy M, Rivollat M, Mendisco F, Pemonge M- H, Coutelier C, Couture C, et al. Distinct ancestries for similar funerary practices? A GIS analysis that compares funerary with osteological and aDNA from the Middle Neolithic necropolis of Gurgy " Les Noisat" (Yonne, France). J Anthropol Sci 2016; in press.

117. Rey L, Goude G, Rottier S. Comportements alimentaires au Néolithique: nouveaux résultats dans le Bassin parisien à partir de l'étude isotopique (δ13C, δ15N) de la nécropole de Gurgy « Les Noisats » (Yonne, Ve millénaire av. J.-C.). Bull Mém Soc Anthropol Paris 2016; in press.

118. Garn SM, Lewis AB, Bonné B. Third molar formation and its development course. The Angle Orthodontist 1962; 32: 270–279.

119. Demirjian A, Goldstein H, Tanner JM. A new system of dental age assessment. Hum Biol 1973; 45: 211–227. PMID: 4714564

120. Molnar S. Human tooth wear, tooth function and cultural variability. Am J Phys Anthropol 1971; 34: 175–190. PMID: 5572602

121. Moorrees CFA, Fanning EA, Hunt EE. Formation and resorption of three deciduous teeth in children. Am J Phys Anthropol 1963; 21: 205–213. PMID: 14110696

122. Moorrees CFA, Fanning EA, Hunt EE. Age variation of formation stages for ten permanent teeth. J Dent Res 1963; 42: 1490–1502. PMID: 14081973

123. Scheuer L, Black S. Developmental juvenile osteology. London: Academic Press; 2000.

124. Schmitt A. Une nouvelle méthode pour estimer l'âge au décès des adultes à partir de la surface sacro-pelvienne iliaque. Bull Mém Soc Anthropol Paris 2005; 17: 1–13.

125. Bruzek J. A method for visual determination of sex, using the human hip bone. Am J Phys Anthropol 2002; 117: 157–168. PMID: 11815949

126. Murail P, Bruzek J, Braga J. A new approach to sexual diagnosis in past populations. Practical adjustments from Van Vark's procedure. Int J Osteoarchaeol 1999; 9: 39–53.

127. Murail P, Bruzek J, Houët F, Cunha E. DSP: a tool for probabilistic sex diagnosis using worldwide variability in hip-bone measurements. Bull Mém Soc Anthropol Paris 2005; 17: 167–176.

128. Bronk Ramsey C, Lee S. Recent and planned developments of the program OxCal. Radiocarbon 2013; 55: 720–730.

129. Reimer PJ, Bard E, Bayliss A, Beck JW, Blackwell PG, Bronk Ramsey C, et al. IntCal13 and marine13 radiocarbon age calibration curves 0–50,000 years cal BP. Radiocarbon 2013; 55: 1869–1887.

130. Spoor F, Zonneveld F, Macho GA. Linear measurements of cortical bone and dental enamel by computed tomography: applications and problems. Am J Phys Anthropol 1993; 91: 469–484. PMID: 8372936

131. Coleman MN, Colbert MW. Technical note: CT thresholding protocols for taking measurements on three-dimensional models. Am J Phys Anthropol 2007; 133: 723–725. PMID: 17326102

132. Smith TM, Olejniczak AJ, Martin LB, Reid DJ. Variation in hominoid molar enamel thickness. J Hum Evol 2005; 48: 575–592. PMID: 15927661

133. Bayle P. Analyses quantitatives par imagerie à haute résolution des séquences de maturation dentaire et des proportions des tissus des dents déciduales chez les Néandertaliens et les Hommes modernes. Thèse de doctorat, Université de Toulouse III—Paul Sabatier. 2008.

134. Bayle P, Braga J, Mazurier A, Macchiarelli R. Brief communication: high-resolution assessment of the dental developmental pattern and characterization of tooth tissue proportions in the late Upper Paleolithic child from La Madeleine, France. Am J Phys Anthropol 2009; 138: 493–498. doi: 10.1002/ajpa.21000 PMID: 19170211

135. Zanolli C, Bondioli L, Coppa A, Dean MC, Bayle P, Candilio F, et al. The late Early Pleistocene human dental remains from Uadi Aalad and Mulhuli-Amo (Buia), Eritrean Danakil: macromorphology and microstructure. J Hum Evol 2014; 74: 96–113. doi: 10.1016/j.jhevol.2014.04.005 PMID: 24852385

136. Le Luyer M, Coquerelle M, Rottier S, Bayle P. 3D models related to the publication: Internal tooth structure and burial practices: insights into the Neolithic necropolis of Gurgy (France, 5100–4000 cal. BC). MorphoMuseuM 2016; 2: e1, doi: 10.18563/m3.2.1.e1

137. Dean MC, Wood BA. A digital radiographic atlas of great apes skull and dentition. In: Bondioli L, Macchiarelli R, editors. Digital archives of human paleobiology. Milan: ADS Solutions; 2003.

138. Macchiarelli R, Mazurier A, Volpato V. L'apport des nouvelles technologies à l'étude des Néandertaliens. In: Vandermeersch B, Maureille B, editors. Les Néandertaliens. Biologie et cultures. Paris: Comité des Travaux Historiques et Scientifiques; 2007. pp. 169–179.

139. Ward JH. Hierarchical grouping to optimize an objective function. Journal of the American Statistical Association 1963; 58: 236–244.

140. Gunz P, Mitteroecker P, Bookstein F. Semilandmarks in three dimensions. In: Slice DE, editor. Modern morphometrics in physical anthropology. New York: Klewer Academic/Plenum; 2005. pp. 73–98.

141. Polychronis G, Christou P, Mavragani M, Halazonetis DJ. Geometric morphometric 3D shape analysis and covariation of human mandibular and maxillary first molars. Am J Phys Anthropol 2013; 152: 186–196. doi: 10.1002/ajpa.22340 PMID: 24009105

142. Coquerelle M, Bookstein FL, Braga J, Halazonetis DJ, Weber GW, Mitteroecker P. Sexual dimorphism of the human mandible and its association with dental development. Am J Phys Anthropol 2011; 145: 192–202. doi: 10.1002/ajpa.21485 PMID: 21365613

143. Gunz P, Mitteroecker P. Semilandmarks: a method for quantifying curves and surfaces. Hystrix 2013; 24: 103–109.

144. Mitteroecker P, Gunz P. Advances in geometric morphometrics. Evol Biol 2009; 36: 235–247.

145. Rohlf FJ, Slice DE. Extensions of the Procrustes method for the optimal superimposition of landmarks. Systematic Biology 1990; 39: 40–59.

146. Bookstein FL. Combining the tools of geometric morphometrics. In: Marcus F, Corti M, Loy A, Naylor GJP, Slice DE, editors. Advances in morphometrics. New York: Plenum Press; 1996. pp. 131–151.

147. R Development Core Team. R: A language and environment for statistical computing. Vienna: R Foundation for Statistical Computing; 2012.

148. Mitteroecker P, Gunz P, Bernhard M, Schaefer K, Bookstein FL. Comparison of cranial ontogenetic trajectories among great apes and humans. J Hum Evol 2004; 46: 679–697. PMID: 15183670

149. Mitteroecker P, Gunz P, Windhager S, Schaefer K. A brief review of shape, form, and allometry in geometric morphometrics, with applications to human facial morphology. Hystrix 2013; 24: 59–66.

150. Thévenet C. Une relecture des pratiques funéraires du Rubané récent et final du Bassin parisien: l'exemple des fosses sépulcrales dans la vallée de l'Aisne. Bull Soc Préhist Fr 2004; 101: 815–826.

151. Dubouloz J. Datation absolue du premier Néolithique du Bassin parisien: complément et relecture des données RRBP et VSG. Bull Soc Préhist Fr 2003; 100: 371–689.

152. Constantin C, Ilett M. Une étape finale dans le Rubané récent du Bassin parisien. In: Jeunesse C, editor. Le Néolithique danubien et ses marges entre Rhin et Seine. Actes du 22e Colloque interrégional sur le Néolithique (27–29 octobre 1995, Strasbourg); 1997. pp. 207–300.

153. Guilaine J. Sépultures d'Occident et genèses des mégalithismes (9000–3500 avant notre ère). Paris: Editions Errance; 1998.

154. Jeunesse C. Pratiques funéraires au néolithique ancien: sépultures et nécropoles des sociétés danubiennes (5500–4900 av. J.-C.). Paris: Editions Errance; 1997.

155. Augereau A, Chambon P. Les occupations néolithiques de Macherin à Monéteau (Yonne). Mémoire de la Société préhistorique française; 2011.

156. Chambon P, Leclerc J. Les tombes multiples dans le Néolithique français: aléa statistique ou pratique institutionnalisée? Bull Soc Préhist Fr 2007; 104: 289–306.

157. Feeney RN. Microtomographic analysis of sexual dimorphism and dental tissue distribution in human molars. PhD dissertation, Ohio Stat University. 2009.

158. Alvesalo L. Sex chromosomes and human growth. A dental approach. Hum Genet 1997; 101: 1–5. PMID: 9385359

159. Alvesalo L, Tammisalo E. Enamel thickness in 45,X females' permanent teeth. Am J Hum Genet 1981; 33: 464–469. PMID: 7246547

160. Alvesalo L, Tammisalo E, Townsend GC. Upper central incisor and canine tooth crown size in 47, XXY males. J Dent Res 1991; 70: 1057–1060. PMID: 2066487

161. Kay RF, Hiiemae KM. Jaw movement and tooth use in recent and fossil primates. Am J Phys Anthropol 1974; 40: 227–256. PMID: 4815136

162.   Macho GA, Berner M. Enamel thickness and the helicoidal occlusal plane. Am J Phys Anthropol 1994; 94: 327–337. PMID: 7943189

163.   Macho GA, Moggi-Cecchi J. Reduction of maxillary molars in *Homo sapiens sapiens*: a different perspective. Am J Phys Anthropol 1992; 87: 151–159. PMID: 1543241

164.   Riga A, Belcastro MG, Moggi-Cecchi J. Environmental stress increases variability in the expression of dental cusps. Am J Phys Anthropol 2014; 153: 397–407. doi: 10.1002/ajpa.22438 PMID: 24264332

165.   Kelley JL, Swanson WJ. Dietary change and adaptive evolution of enamelin in humans and among primates. Genetics 2008; 178: 1595–1603. doi: 10.1534/genetics.107.077123 PMID: 18245370